The Viscomagnetic Effect in Mixtures

A. L. J. Burgmans *, P. G. van Ditzhuyzen, and H. F. P. Knaap

Kamerlingh Onnes Laboratorium, Rijksuniversiteit, Leiden

(Z. Naturforsch. **28 a**, 849–861 [1973]; received 6th March 1973)

Dedicated to Prof. Dr. L. Waldmann on the occasion of his 60th birthday

A study is presented of the viscomagnetic effect in binar mixtures consisting of diatomics and noble gas atoms. The following systems have been investigated: HD–He, HD–Ne, HD–Ar and N_2–He, N_2–Ne, N_2–Ar. The purpose of this research is to obtain effective cross sections for the relatively simple interaction between monatomic and diatomic molecules. Various effective cross sections are presented.

1. Introduction

In a preceeding article [1] experiments have been reported on the temperature dependence of the magnetic field effect on viscosity in pure gases consisting of nonspherical molecules. In this chapter we will present results obtained from similar experiments on mixtures of polyatomic gases with noble gases.

The shear viscosity of a gas of polyatomic molecules in a magnetic field can be described by five independent coefficients, i. e., according to the notation of Coope and Snider [2]: η_0^+, η_1^+, η_2^+, η_1^- and η_2^- (see also Ref. [3]). Theoretical expressions for these coefficients can be obtained from a Chapman-Enskog treatment of the field effect [4], in which the nonequilibrium distribution function is expanded in terms of irreducible tensors made up of reduced velocity $\boldsymbol{W}$ and angular momentum $\boldsymbol{J}$. From the experiments it is seen that in simple gases [5–7] and in mixtures of these gases with noble gases [8] the field effect on viscosity is dominated by one type of angular momentum polarization only, viz. $[\boldsymbol{J}]^{(2)}$. Hence the experimental results can be characterized by two parameters, one for the magnitude of the viscosity change and one for the field strength at which the effect occurs. These quantities are related to collision integrals, which are determined mainly by the anisotropic interaction between molecules. Consequently these experiments provide direct information about the non spherical part of the molecular interaction.

Because the interaction between non spherical and spherical particles is simpler to describe than the interaction between two non spherical particles we have extended our investigations to mixtures of polyatomic gases (non spherical) with noble gases (spherical). In order to test non-spherical potentials which describe such interactions, one needs information on the collision integrals over a large temperature range. For this reason experiments have been performed as a function of temperature.

The systems HD – He, HD – Ne, HD – Ar, N_2 – He, N_2 – Ne and N_2 – Ar have been investigated both at 77 K and 293 K. The field effect for each system has been studied as a function of the noble gas fraction by performing experiments at various compositions.

2. Theory

On pure gases extensive theoretical work has been done concerning the magnetic field effects on transport properties. For a survey see Ref. [9]. For mixtures consisting of linear diatomic molecules, a classical treatment of the shear viscosity tensor is given by Tip [10]. More recently a formal theory for mixtures was given by Raum and Köhler [11], based on the Waldmann-Snider kinetic equation. In the calculations of Ref. [10] the contribution of the dominant $[\boldsymbol{J}]^{(2)}$ polarization has been considered. Explicit expressions are given for the viscosity coefficients of binary mixtures in which one of the components is a noble gas. For such systems the field effect is found to be the same as for pure gases, and for the coefficients measured in our experimental situation, the functional form is given by:

$$\frac{\eta_1^+ + \eta_2^+ - 2\,\eta(0)}{2\,\eta(0)} = -\frac{1}{2}\,\Psi_{02}\left[\frac{\xi_{02}^2}{1+\xi_{02}^2} + \frac{4\,\xi_{02}^2}{1+4\,\xi_{02}^2}\right] \tag{1}$$

where $\eta(0)$ is the field free viscosity of the gas mixture. The expressions for ξ_{02} and Ψ_{02} are, however,

Reprint requests to Dr. H. F. P. Knaap, Kamerlingh Onnes Laboratorium, Nieuwsteeg 18, *Leiden*, The Netherlands.

* Present address: Texas A and M University, College Station, *Texas*, U.S.A.

more complicated than for pure gases. The shape of the curve given by this expression as a function of ξ_{02} (or H/p) has a dispersion-like character reaching saturation for high values of ξ_{02}.

2.1. Position of the effect on the H/p axis

The quantity ξ_{02} fixes the position of the effect on the H/p axis and is determined by the decay of the tensorial polarization, $[\boldsymbol{J}_A]^{(2)}$. The subscript A is used here to denote the molecular species upon which experiments are performed. In pure polyatomic gases the decay of this polarization is a consequence of collisions between identical molecules and can be expressed by the reorientation cross section for tensorial polarization, $\mathfrak{S}(02)_A$. The subscript A now refers to the interactions ** which are taking place in a pure gas consiting only of molecules A. In mixtures with a noble gas (component B) the decay of $[\boldsymbol{J}_A]^{(2)}$ polarization may result from two kinds of interactions: collisions of the type A – A and of the type A – B. The decay through the interaction A – B is expressed by a cross section, denoted as $\mathfrak{S}\left(\begin{smallmatrix}02A\\02A\end{smallmatrix}\right)_{AB}$. The A between the brackets refers to the polarization of the polyatomic molecule considered, while the subscript AB refers to the interaction. For the proper definition of $\mathfrak{S}\left(\begin{smallmatrix}02A\\02A\end{smallmatrix}\right)_{AB}$ see Table 1, in which the cross sections are defined (see e. g. Refs. [1] and [13]). The expression for ξ_{02} can be written [10] in terms of the cross sections $\mathfrak{S}(02)_A$ and $\mathfrak{S}\left(\begin{smallmatrix}02A\\02A\end{smallmatrix}\right)_{AB}$:

$$\xi_{02} = \{x_A \langle v_A \rangle_0 \mathfrak{S}(02)_A + x_B \langle v_{AB} \rangle_0 \mathfrak{S}\left(\begin{smallmatrix}02A\\02A\end{smallmatrix}\right)_{AB}\}^{-1} \cdot \frac{g \mu_N k T}{\hbar} \frac{H}{p}, \quad (2)$$

where x_A and x_B are the mole fractions of the two components ($x_A + x_B = 1$). The mean relative velocities are given by:

$$\langle v_A \rangle_0 = (8 k T/\pi \mu_A)^{1/2}$$
$$\text{and} \qquad \langle v_{AB} \rangle_0 = (8 k T/\pi \mu_{AB})^{1/2} \quad (3)$$

with μ_A and μ_{AB} the reduced masses which are $m_A/2$ and $m_A m_B/(m_A + m_B)$, respectively. The quantity g is the molecular g-factor and μ_N the nuclear magneton. The other symbols have their usual meaning. From the experiments one determines the $(H/p)_{1/2}$ value, that is the value of H/p for which the effect reaches half saturation. This is given by [see also Equation (1)]:

$$(H/p)_{1/2} = (2^{1/2} g \mu_N k T/\hbar)^{-1} \{x_A \langle v_A \rangle_0 \mathfrak{S}(02)_A + x_B \langle v_{AB} \rangle_0 \mathfrak{S}\left(\begin{smallmatrix}02A\\02A\end{smallmatrix}\right)_{AB}\}. \quad (4)$$

Thus theory predicts a linear behaviour of the $(H/p)_{1/2}$ values versus the noble gas mole fraction x_B.

2.2. The magnitude of the field effect

The magnitude of the field effect on viscosity, described by Ψ_{02}, is mainly determined by the strength of the coupling between the anisotropies in the angular momentum space and in the velocity space. In pure gases this coupling is characterized by the cross section $\mathfrak{S}\left(\begin{smallmatrix}02\\20\end{smallmatrix}\right)_A$ which describes the production of $[\boldsymbol{J}_A]^{(2)}$ polarization from a $[\boldsymbol{W}_A]^{(2)}$ polarization through the interaction of the type A – A (see also earlier footnote). The quantity Ψ_{02} is in this case given by:

$$\Psi_{02} = \mathfrak{S}\left(\begin{smallmatrix}02\\20\end{smallmatrix}\right)_A^2 / \mathfrak{S}(02)_A \mathfrak{S}(20)_A \text{ (pure gases)}, \quad (5)$$

where $\mathfrak{S}(20)_A$ is the gas-kinetic cross section which can be obtained from the field free viscosity $\eta_A(0)$. In binary mixtures of polyatomic gases (A) with noble gases (B) the quantity Ψ_{02} is much more complicated. Now a tensor polarization $[\boldsymbol{J}_A]^{(2)}$ can be produced in different ways, viz.: a) from a $[\boldsymbol{W}_A]^{(2)}$ polarization through collisions of the type A – A, b) from a $[\boldsymbol{W}_A]^{(2)}$ polarization through collisions A – B and c) from a $[\boldsymbol{W}_B]^{(2)}$ polarization through collisions A – B. These three production mechanisms of $[\boldsymbol{J}_A]^{(2)}$ polarization can be described respectively by the cross sections $\mathfrak{S}\left(\begin{smallmatrix}02\\20\end{smallmatrix}\right)_A$, $\mathfrak{S}\left(\begin{smallmatrix}02A\\20A\end{smallmatrix}\right)_{AB}$ and $\mathfrak{S}\left(\begin{smallmatrix}02A\\20B\end{smallmatrix}\right)_{AB}$. The last two cross sections are not independent, as can be readily seen by performing the average over the center of mass velocities. This results in the relation

$$\mathfrak{S}\left(\begin{smallmatrix}02A\\20B\end{smallmatrix}\right)_{AB} = (m_A/m_B)\, \mathfrak{S}\left(\begin{smallmatrix}02A\\20A\end{smallmatrix}\right)_{AB}, \quad (6)$$

where m_A and m_B are the masses of the molecules. Hence the magnitude of the field effect is essentially determined by two cross sections which couple the polarization in velocity space to the polarization in the angular momentum space. The expression for Ψ_{02} is given in Ref. [10] and can be written in terms of these cross sections

** In discussions for which only pure gases are considered script A is dropped (see e. g. Ref. 12 and the appendix of Ref. 7).

Table 1. Definition of the cross sections used in this paper

for pure polyatomic gases (A)

$$\mathfrak{S}(20)_{\mathrm{A}} = \frac{1}{\langle v_{\mathrm{A}}\rangle_0}\,\frac{\langle [W_{\mathrm{A}}]^{(2)} : R_0[W_{\mathrm{A}}]^{(2)}\rangle_0}{\langle [W_{\mathrm{A}}]^{(2)} : [W_{\mathrm{A}}]^{(2)}\rangle_0}\,; \qquad \mathfrak{S}(02)_{\mathrm{A}} = \frac{1}{\langle v_{\mathrm{A}}\rangle_0}\,\frac{\langle [J_{\mathrm{A}}]^{(2)} : R_0[J_{\mathrm{A}}]^{(2)}\rangle_0}{\langle [J_{\mathrm{A}}]^{(2)} : [J_{\mathrm{A}}]^{(2)}]\rangle_0}$$

$$\mathfrak{S}\binom{02}{20}_{\mathrm{A}} = \frac{1}{\langle v_{\mathrm{A}}\rangle_0}\,\frac{\langle [J_{\mathrm{A}}]^{(2)} : R_0[W_{\mathrm{A}}]^{(2)}\rangle_0}{\langle [J_{\mathrm{A}}]^{(2)} : [J_{\mathrm{A}}]^{(2)}\rangle_0^{1/2}\langle [W_{\mathrm{A}}]^{(2)} : [W_{\mathrm{A}}]^{(2)}\rangle_0^{1/2}}$$

where

$$R_0\,\Phi = -(2\pi)^4\hbar^2 n^{-1}\,\mathrm{tr}_1 \int \mathrm{d}\boldsymbol{p}_1 f_1^{(0)} \left\{ \int t_{g'}^{g}\,(\Phi' + \Phi_1')\; t_{g'}^{g+}\delta(E)\;\mathrm{d}\boldsymbol{p}' + \right.$$
$$\left. - \frac{\mathrm{i}}{2\pi}\,[t_g^g\,(\Phi+\Phi_1) - (\Phi+\Phi_1)\; t_g^{g+}] \right\},\ \text{see Ref. 14.}$$

for mixtures of a polyatomic gas (A) and a noble gas (B)

$$\mathfrak{S}\binom{20\mathrm{A}}{20\mathrm{A}}_{\mathrm{AB}} = \frac{1}{\langle v_{\mathrm{AB}}\rangle_0}\,\frac{\langle [W_{\mathrm{A}}]^{(2)} : R_0^{\mathrm{AB}}[W_{\mathrm{A}}]^{(2)}\rangle_0}{\langle [W_{\mathrm{A}}]^{(2)} : [W_{\mathrm{A}}]^{(2)}\rangle_0}\,;$$

$$\mathfrak{S}\binom{20\mathrm{B}}{20\mathrm{B}}_{\mathrm{AB}} = \frac{1}{\langle v_{\mathrm{AB}}\rangle_0}\,\frac{\langle [W_{\mathrm{B}}]^{(2)} : R_0^{\mathrm{AB}}[W_{\mathrm{B}}]^{(2)}\rangle_0}{\langle [W_{\mathrm{B}}]^{(2)} : [W_{\mathrm{B}}]^{(2)}\rangle_0}\,;$$

$$\mathfrak{S}\binom{20\mathrm{A}}{20\mathrm{B}}_{\mathrm{AB}} = \frac{1}{\langle v_{\mathrm{AB}}\rangle_0}\,\frac{\langle [W_{\mathrm{A}}]^{(2)} : R_0^{\mathrm{AB}}[W_{\mathrm{B}}]^{(2)}\rangle_0}{\langle [W_{\mathrm{A}}]^{(2)} : [W_{\mathrm{A}}]^{(2)}\rangle_0^{1/2}\langle [W_{\mathrm{B}}]^{(2)} : [W_{\mathrm{B}}]^{(2)}\rangle_0^{1/2}}\,;$$

$$\mathfrak{S}\binom{02\mathrm{A}}{02\mathrm{A}}_{\mathrm{AB}} = \frac{1}{\langle v_{\mathrm{AB}}\rangle_0}\,\frac{\langle [J_{\mathrm{A}}]^{(2)} : R_0^{\mathrm{AB}}[J_{\mathrm{A}}]^{(2)}\rangle_0}{\langle [J_{\mathrm{A}}]^{(2)} : [J_{\mathrm{A}}]^{(2)}\rangle_0}\,;$$

$$\mathfrak{S}\binom{02\mathrm{A}}{20\mathrm{A}}_{\mathrm{AB}} = \frac{1}{\langle v_{\mathrm{AB}}\rangle_0}\,\frac{\langle [J_{\mathrm{A}}]^{(2)} : R_0^{\mathrm{AB}}[W_{\mathrm{A}}]^{(2)}\rangle_0}{\langle [J_{\mathrm{A}}]^{(2)} : [J_{\mathrm{A}}]^{(2)}\rangle_0^{1/2}\langle [W_{\mathrm{A}}]^{(2)} : [W_{\mathrm{A}}]^{(2)}\rangle_0^{1/2}}\,;$$

$$\mathfrak{S}\binom{02\mathrm{A}}{20\mathrm{B}}_{\mathrm{AB}} = \frac{1}{\langle v_{\mathrm{AB}}\rangle_0}\,\frac{\langle [J_{\mathrm{A}}]^{(2)} : R_0^{\mathrm{AB}}[W_{\mathrm{B}}]^{(2)}\rangle_0}{\langle [J_{\mathrm{A}}]^{(2)} : [J_{\mathrm{A}}]^{(2)}\rangle_0^{1/2}\langle [W_{\mathrm{B}}]^{(2)} : [W_{\mathrm{B}}]^{(2)}\rangle_0^{1/2}}\,;$$

where

$$R_0^{\mathrm{AB}}\Phi = -(2\pi)^4\hbar^2 n_{\mathrm{B}}^{-1}\,\mathrm{tr}_{\mathrm{B}} \int \mathrm{d}\boldsymbol{p}_{\mathrm{B}}\, f_{\mathrm{B}}^{(0)} \{ \int t_{g'\,\mathrm{AB}}^{g\,\mathrm{AB}}\,(\Phi')\; t_{g'\,\mathrm{AB}}^{g+\mathrm{AB}}\delta(E)\;\mathrm{d}\boldsymbol{p}_{\mathrm{B}}' +$$
$$- \frac{i}{2\pi}\,[t_{g\,\mathrm{AB}}^{g\,\mathrm{AB}}\,(\Phi) - (\Phi)\; t_{g\,\mathrm{AB}}^{g+\mathrm{AB}}]\},\ \text{see also Ref. 11.}$$

$$\Psi_{02} = x_{\mathrm{A}}\,\frac{\{x_{\mathrm{A}}\langle v_{\mathrm{A}}\rangle_0 B_{\mathrm{A}}{}^{20}\,\mathfrak{S}\binom{02}{20}_{\mathrm{A}} + x_{\mathrm{B}}\langle v_{\mathrm{AB}}\rangle_0\,[B_{\mathrm{A}}{}^{20} + (m_{\mathrm{A}}/m_{\mathrm{B}})\,B_{\mathrm{B}}{}^{20}]\,\mathfrak{S}\binom{02\mathrm{A}}{20\mathrm{A}}_{\mathrm{AB}}\}^2}{2\{x_{\mathrm{A}}\langle v_{\mathrm{A}}\rangle_0\,\mathfrak{S}(02)_{\mathrm{A}} + x_{\mathrm{B}}\langle v_{\mathrm{AB}}\rangle_0\,\mathfrak{S}\binom{02\mathrm{A}}{02\mathrm{A}}_{\mathrm{AB}}\}\{x_{\mathrm{A}}B_{\mathrm{A}}{}^{20} + x_{\mathrm{B}}B_{\mathrm{B}}{}^{20}\}}\,. \tag{7}$$

Here $B_{\mathrm{A}}{}^{20}$ and $B_{\mathrm{B}}{}^{20}$ are functions of gas-kinetic cross sections which determine the field free viscosity of the mixture, and are given by:

$$B_{\mathrm{A}}{}^{20} = (25/2)\; x_{\mathrm{A}}\,x_{\mathrm{B}}\{x_{\mathrm{B}}\langle v_{\mathrm{B}}\rangle_0\,\mathfrak{S}(20)_{\mathrm{B}} + \langle v_{\mathrm{AB}}\rangle_0\,[x_{\mathrm{A}}\,\mathfrak{S}\binom{20\mathrm{B}}{20\mathrm{B}}_{\mathrm{AB}} - x_{\mathrm{B}}\,\mathfrak{S}\binom{20\mathrm{A}}{20\mathrm{B}}_{\mathrm{AB}}]\}/d$$

and

$$B_{\mathrm{B}}{}^{20} = (25/2)\; x_{\mathrm{A}}\,x_{\mathrm{B}}\{x_{\mathrm{A}}\langle v_{\mathrm{A}}\rangle_0\,\mathfrak{S}(20)_{\mathrm{A}} + \langle v_{\mathrm{AB}}\rangle_0\,[x_{\mathrm{B}}\,\mathfrak{S}\binom{20\mathrm{A}}{20\mathrm{A}}_{\mathrm{AB}} - x_{\mathrm{A}}\,\mathfrak{S}\binom{20\mathrm{A}}{20\mathrm{B}}_{\mathrm{AB}}]\}/d\,, \tag{8}$$

where

$$d = (25/4)\; x_{\mathrm{A}}\,x_{\mathrm{B}}\{x_{\mathrm{A}}\langle v_{\mathrm{A}}\rangle_0\,\mathfrak{S}(20)_{\mathrm{A}} + x_{\mathrm{B}}\langle v_{\mathrm{AB}}\rangle_0\,\mathfrak{S}\binom{20\mathrm{A}}{20\mathrm{A}}_{\mathrm{AB}}\}$$
$$\cdot\{x_{\mathrm{B}}\langle v_{\mathrm{B}}\rangle_0\,\mathfrak{S}(20)_{\mathrm{B}} + x_{\mathrm{A}}\langle v_{\mathrm{AB}}\rangle_0\,\mathfrak{S}\binom{20\mathrm{B}}{20\mathrm{B}}_{\mathrm{AB}}\} - (25/4)\; x_{\mathrm{A}}{}^2\,x_{\mathrm{B}}{}^2\langle v_{\mathrm{AB}}\rangle_0{}^2\,\mathfrak{S}\binom{20\mathrm{A}}{20\mathrm{B}}_{\mathrm{AB}}\,.$$

Note that if only component A is present, Eqs. (2) and (7) reduce to the expressions which describe the field effect in pure gases.

3. Experiment

To measure the magnetic field effect on the viscosity in mixtures we use apparatus I described in Ref. [1]. In principle the apparatus is a Wheatstone bridge for gasflow, see Fig. 1, in which one of the circular capillaries is placed between the poles of a magnet (Oerlikon C 3) perpendicular to the field direction. Starting from a steady state situation the magnetic field is switched on, causing a change in

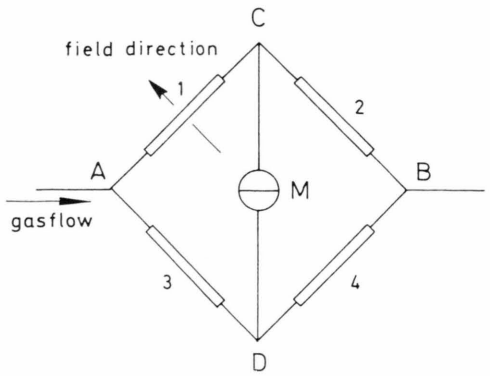

Fig. 1. Schematic diagram of the capillary bridge.

the viscosity in capillary 1. Consequently a pressure difference $p_C - p_D$ appears which is measured with the differential capacitance manometer (M) having a sensitivity of better than 10^{-5} Torr (Varian MMM). This pressure difference is related to a combination of viscosity coefficients [15] which can be calculated from:

$$-\frac{\eta_1^+ + \eta_2^+ - 2\,\eta(0)}{2\,\eta(0)} = 4\,\frac{p_C - p_D}{p_A - p_B}\,f\,, \qquad (9)$$

where f a correction factor of the order unity given by:

$$f = \frac{2\,(p_C + K_\alpha)}{(p_A + K_\alpha) + (p_B + K_\alpha)} \cdot \left[1 + \frac{1}{16}\,\frac{R}{l}\,\mathrm{Re}\left(1 + \ln\frac{p_A}{p_C}\right)\right]\left(1 + \frac{K_\beta}{p}\right). \qquad (10)$$

This factor has been discussed in detail in Ref. [1] and is constructed from three different parts:

a) $2\,(p_C + K_\alpha)/[\,(p_A + K_\alpha) + (p_B + K_\alpha)\,]$ which corrects for the expansion of the gas and Knudsen effects on the field free flow, and usually has a value of about 1.3. The quantity K_α is calculated from $K_\alpha = n_\alpha\, p\, \xi/R$, where $p = \frac{1}{2}\,(p_A + p_C)$ and R the radius of the capillary. For n_α the value 4 is used in accordance with Ref. [16] while ξ is the mean free path of the molecules given by $x_A\,\xi_A + x_B\,\xi_B$, where ξ_A and ξ_B are the mean free pathes of molecules A and B. For a binary mixture they are given by Chapman and Cowling [17]:

$$\xi_A^{-1} = 2^{1/2}\,\pi\, n_A\, \sigma_A^2 + \pi\, n_B\, \sigma_{AB}^2\,(1 + m_A/m_B)^{1/2}$$

and (11)

$$\xi_B^{-1} = 2^{1/2}\,\pi\, n_B\, \sigma_B^2 + \pi\, n_A\, \sigma_{AB}^2\,(1 + m_B/m_A)^{1/2}$$

where n_A and n_B are the number densities and σ_{AB} is the average value of the molecular diameters σ_A and σ_B.

b) $[1 + (1/16)\,(R/l)\,\mathrm{Re}\{1 + \ln(p_A/p_C)\}]$ takes into account additional pressure losses at the entrance of the capillary and also in the capillary. The correction is usually small, having a value between 1 and 1.01. The quantity l is the length of the capillary, and Re is Reynolds number.

c) $1 + K_\beta/p$ corrects for Knudsen effects in the magnitude of the field effect.

The H/p values are also affected by Knudsen effects [6] and the correction is given by:

$$H/p = (H/p)_{\exp}/(1 + K_\gamma/p)\,. \qquad (12)$$

The quantities K_β and K_γ are determined experimentally by extrapolating to infinite pressure. Analogous to K_α, these quantities can be written as

$$K_{\beta,\gamma} = n_{\beta,\gamma}\, p\, \xi_A/R\,.$$

For the mixtures investigated, the numbers n_β and n_γ are found to be the same as for the pure gases [1],

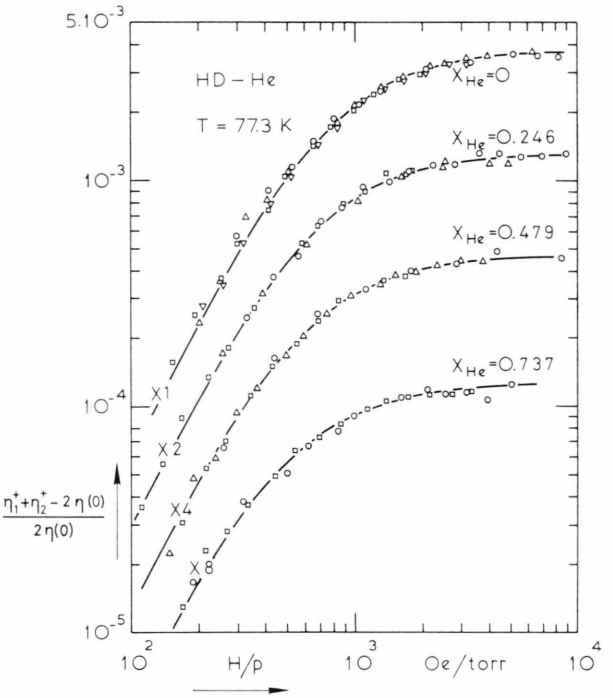

Fig. 2. $-[\eta_1^+ + \eta_2^+ - 2\,\eta(0)]/2\,\eta(0)$ versus H/p for various compositions of the system HD – He at 77.3 K. To distinguish the four different curves for $x_{He} = 0$; 0.246; 0.479 and 0.737, they are vertically shifted by dividing them respectively by 1, 2, 4 and 8.
$x_{He} = 0$: ○ 3.48 torr; △ 4.65 torr; ▽ 9.45 torr; □ 15.7 torr.
$x_{He} = 0.246$: ○ 2.50 torr; △ 7.66 torr; □ 17.9 torr.
$x_{He} = 0.737$: ○ 4.65 torr; △ 8.16 torr; □ 18.6 torr.
$x_{He} = 0.737$: ○ 4.65 torr; □ 9.03 torr.
—— theoretical H/p dependence, scaled to the experimental points.

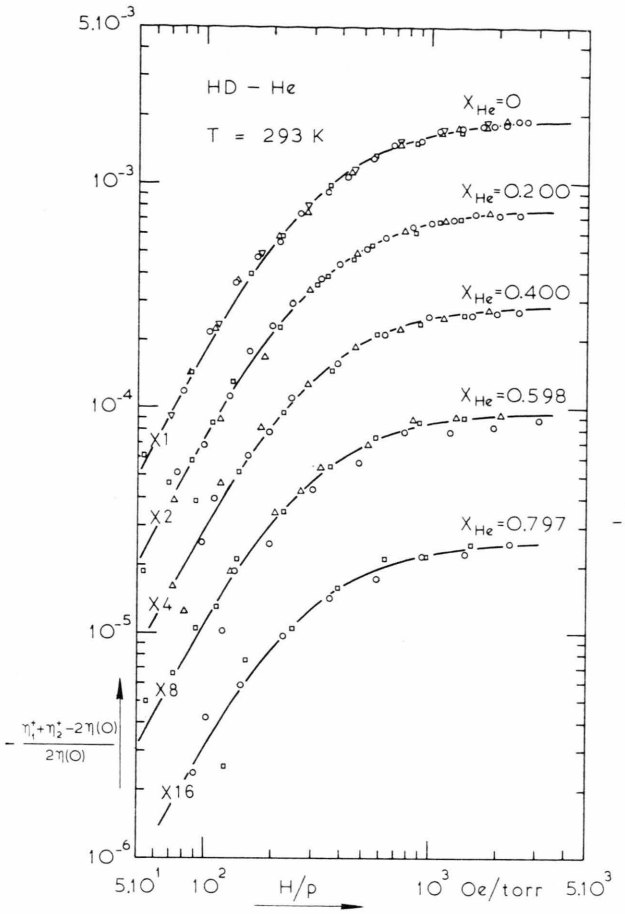

Fig. 3. $-[\eta_1^+ + \eta_2^+ - 2\,\eta\,(0)]/2\,\eta\,(0)$ versus H/p for various compositions of the system HD – He at 293 K. To distinguish the different curves, they are shifted in the vertical directions as in Figure 2.

$x_{He}=0$: ○ 9.76 torr; △ 12.4 torr; ▽ 15.6 torr; □ 20.8 torr.
$x_{He}=0.200$: ○ 10.6 torr; △ 15.1 torr; □ 21.1 torr.
$x_{He}=0.400$: ○ 10.8 torr; △ 15.3 torr; □ 20.1 torr.
$x_{He}=0.598$: ○ 8.28 torr; △ 13.1 torr; □ 20.1 torr.
$x_{He}=0.797$: ○ 11.9 torr; □ 18.3 torr.
—— theoretical H/p dependence, scaled to the experimental points.

i. e., $n_\beta = 10$ and $n_\gamma = 14$ for the HD-noble gas mixtures and $n_\beta = 10$ and $n_\gamma = 3$ for the N_2-noble gas mixtures.

The gases used are obtainend commercially, except HD which is prepared as described in Reference [1]. In all cases mixtures are made by simply dilutinig the polyatomic gas with noble gas. The mole fractions are obtained by assuming that the perfect gas law is valid.

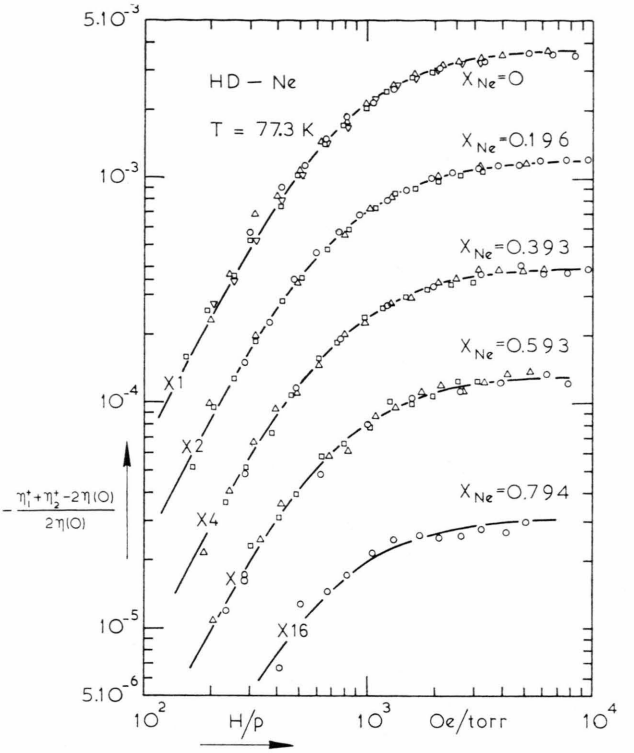

Fig. 4. $-[\eta_1^+ + \eta_2^+ - 2\,\eta\,(0)]/2\,\eta\,(0)$ versus H/p for various compositions of the system HD – Ne at 77.3 K. To distinguish the different curves, they are shifted in the vertical direction as in Figure 2.

$x_{Ne}=0$: ○ △ ▽ □ points taken from Fig. 2.
$x_{Ne}=0.196$: ○ 2.99 torr; △ 5.89 torr; □ 9.28 torr.
$x_{Ne}=0.393$: ○ 2.93 torr; △ 4.94 torr; □ 10.3 torr.
$x_{Ne}=0.593$: ○ 3.68 torr; △ 5.63 torr; □ 9.80 torr.
$x_{Ne}=0.794$: ○ 5.74 torr.
—— theoretical H/p dependence, scaled to the experimental points.

4. Experimental Results and Discussion

Experiments have been performed on the systems: HD – He, HD – Ne, HD – Ar, N_2 – He, N_2 – Ne and N_2 – Ar at 77 K and 293 K. The field effect is obtainend as a function of the mole fraction of the noble gas by measuring various compositions of each system. The results are shown in Figures 2 to 13. The theoretical curves are given by Eq. (1) using ξ_{02} and Ψ_{02} as adaptable parameters for the position along the H/p axis and the magnitude of the effect. It is seen that in all cases the experiments can be described very well by this theoretical expression.

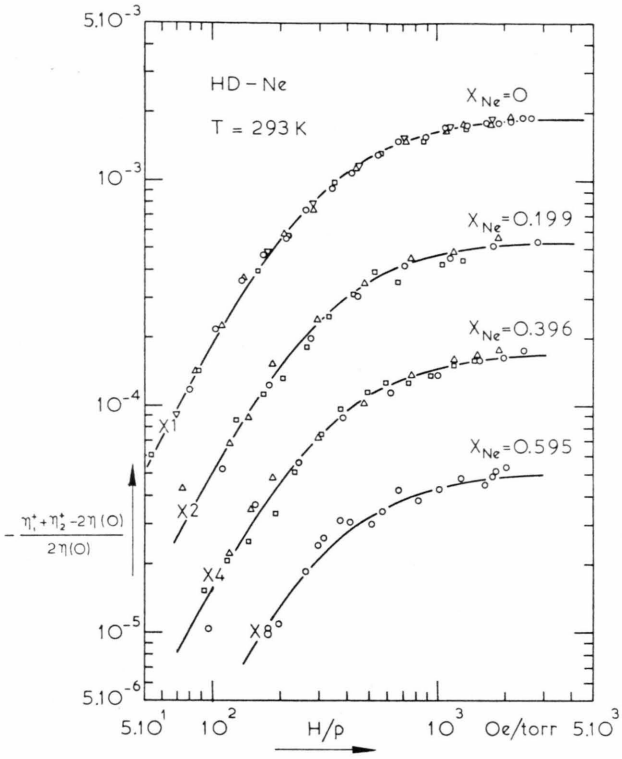

Fig. 5. $-[\eta_1^+ + \eta_2^+ - 2\eta(0)]/2\eta(0)$ versus H/p for various compositions of the system HD – Ne at 293 K. To distinguish the different curves, they are shifted in the vertical direction as in Figure 2.

$x_{Ne}=0$: ○ △ ▽ □ points taken from Fig. 3.
$x_{Ne}=0.199$: ○ 9.12 torr; △ 14.7 torr; □ 21.9 torr.
$x_{Ne}=0.396$: ○ 10.7 torr; △ 14.8 torr; □ 19.3 torr.
$x_{Ne}=0.595$: ○ 13.6 torr.
—— theoretical H/p dependence, scaled to the experimental points.

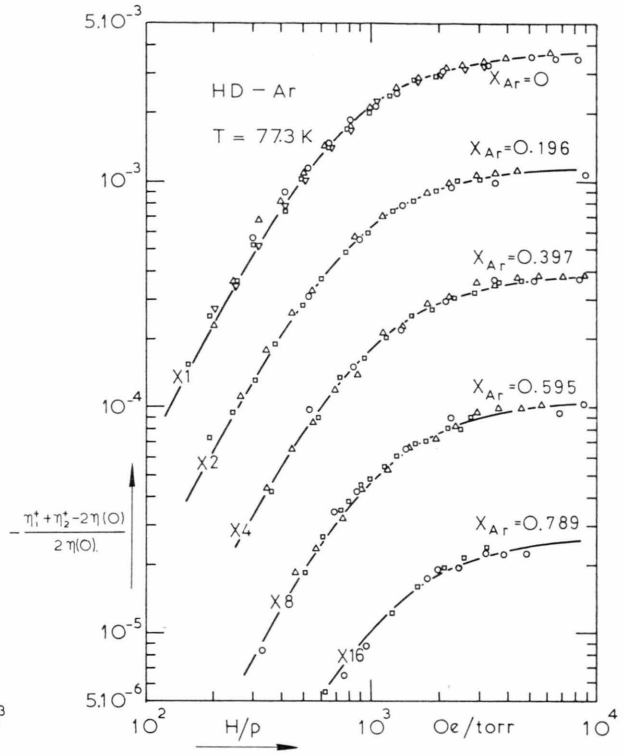

Fig. 6. $-[\eta_1^+ + \eta_2^+ - 2\eta(0)]/2\eta(0)$ versus H/p for various compositions of the system HD – Ar at 77.3 K. To distinguish the different curves, they are shifted in the vertical direction as in Figure 2.

$x_{Ar}=0$: ○ △ ▽ □ points taken from Fig. 2.
$x_{Ar}=0.196$: ○ 1.45 torr; △ 3.26 torr; □ 7.92 torr.
$x_{Ar}=0.397$: ○ 2.65 torr; △ 3.25 torr; □ 6.54 torr.
$x_{Ar}=0.595$: ○ 2.56 torr; △ 5.12 torr; □ 7.71 torr.
$x_{Ar}=0.789$: ○ 2.94 torr; □ 4.61 torr.
—— theoretical H/p dependence, scaled to the experimental points.

4.1. The $(H/p)_{1/2}$ value as a function of composition

In Figs. 14 to 17 the $(H/p)_{1/2}$ values are plotted as a function of the mole fraction of the noble gas. Within the experimental accuracy it is found that for all systems the dependence is linear, as predicted by theory [see Equation (4)]. The cross section $\mathfrak{S}(^{02A}_{02A})_{AB}$ is obtainend from the $(H/p)_{1/2}$ value extrapolated to infinite dilution of the polyatomic molecules ($x_B = 1$). In this limit the polyatomic molecules are surrounded by noble gas atoms so that reorientation occurs only through interactions of the type A – B. The values for $\mathfrak{S}(^{02A}_{02A})_{AB}$ determined in this way are given in Table 2, together with $\mathfrak{S}(02)_A$ as obtained from the experiments on the pure polyatomic gas [1].

It is seen from these values that the heavier or larger the noble gas atoms, the more effective they are in annihilating the $[\boldsymbol{J}_A]^{(2)}$ polarization in the angular momenta of the non spherical molecules. For this reorientation process, collisions between N_2 an Ar are as effective as collisions with other N_2 molecules, as can be seen by comparing the values for $\mathfrak{S}(02)_{N_2}$ and $\mathfrak{S}(^{02N_2}_{02N_2})_{N_2-Ar}$. For pure HD at both temperatures the reorientation cross section $\mathfrak{S}(02)_{HD}$ lies between

$$\mathfrak{S}(^{02HD}_{02HD})_{HD-He} \quad \text{and} \quad (\mathfrak{S}^{02HD}_{02HD})_{HD-Ne}.$$

For the N_2-noble gas mixtures, $\mathfrak{S}(^{02N_2}_{02N_2})_{N_2\text{-n.g.}}$ increases with decreasing temperature, while for the HD-noble gas mixtures this is only the case for $\mathfrak{S}(^{02HD}_{02HD})_{HD-Ar}$.

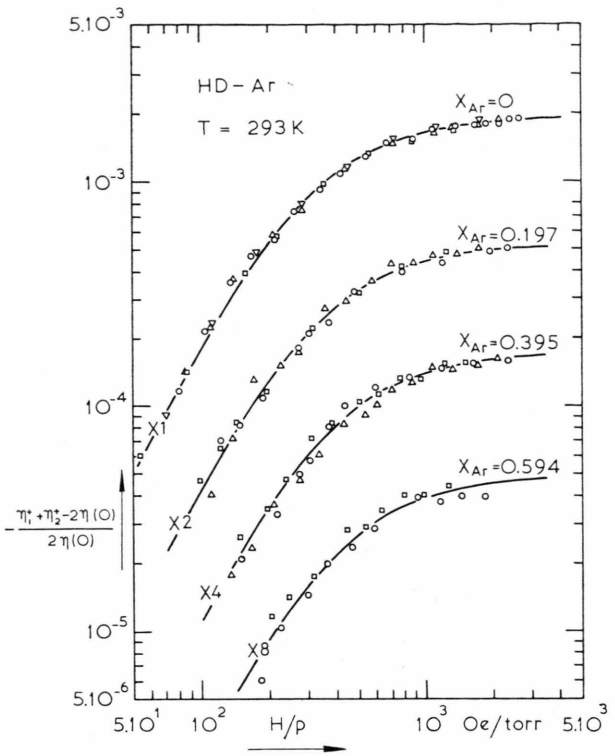

Fig. 7. $-[\eta_1^+ + \eta_2^+ - 2\,\eta(0)]/2\,\eta(0)$ versus H/p for various compositions of the system HD – Ar at 293 K. To distinguish the different curves, they are shifted in the vertical direction as in Figure 2.

$x_{Ar}=0$: ○ △ ▽ □ points taken from Fig. 3.
$x_{Ar}=0.197$: ○ 11.3 torr; △ 16.1 torr; □ 23.2 torr.
$x_{Ar}=0.395$: ○ 11.4 torr; △ 12.9 torr; □ 18.8 torr.
$x_{Ar}=0.594$: ○ 11.7 torr; □ 18.3 torr.
—— theoretical H/p dependence, scaled to the experimental points.

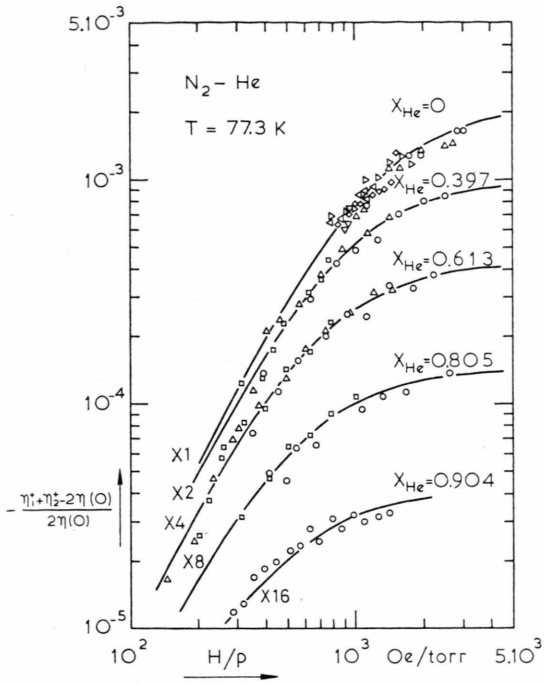

Fig. 8. $-[\eta_1^+ + \eta_2^+ - 2\,\eta(0)]/2\,\eta(0)$ versus H/p for various compositions of the system N_2 – He at 77.3 K. To distinguish the different curves, they are shifted in the vertical direction as in Figure 2.

$x_{He}=0$: ○ 0.966 torr; △ 1.09 torr; ▷ 1.72 torr; ◇ 2.04 torr; ◁ 2.48 torr; ▽ 3.29 torr; □ 5.08 torr.
$x_{He}=0.397$: ○ 1.21 torr; △ 2.19 torr; □ 4.02 torr.
$x_{He}=0.613$: ○ 1.35 torr; △ 2.06 torr; □ 3.94 torr.
$x_{He}=0.805$: ○ 1.14 torr; □ 2.46 torr.
$x_{He}=0.904$: ○ 1.98 torr.
—— theoretical H/p dependence, scaled to the experimental points.

Table 2.

HD-noble gas mixtures	$\mathfrak{S}\binom{02HD}{02HD}$ HD-n.g. (Å²)		$\mathfrak{S}\binom{02HD}{20HD}$ HD-n.g. (Å²)	
	77.3 K	293 K	77.3 K	293 K
HD–He	1.7 ± 0.1	2.1 ± 0.1	0.20 ± 0.01	0.14 ± 0.01
HD–Ne	3.3 ± 0.2	3.3 ± 0.3	0.65 ± 0.04	0.32 ± 0.02
HD–Ar	6.4 ± 0.3	4.9 ± 0.3	1.3 ± 0.1	0.59 ± 0.05
	$\mathfrak{S}(02)_{HD}$ (Å²)		$\mathfrak{S}\binom{02}{20}_{HD}$ (Å²)	
HD	2.95 ± 0.08	2.26 ± 0.07	0.519 ± 0.017	0.282 ± 0.009

N_2-noble gas mixtures	$\mathfrak{S}\binom{02N_2}{02N_2}_{N_2}$-n.g. (Å²)		$\mathfrak{S}\binom{02N_2}{20N_2}_{N_2}$-n.g. (Å²)	
	77.3 K	293 K	77.3 K	293 K
N_2–He	8.3 ± 0.9	5.6 ± 0.3	0.14 ± 0.01	0.080 ± 0.008
N_2–Ne	26 ± 2	15 ± 0.7	0.96 ± 0.1	0.54 ± 0.05
N_2–Ar	55 ± 6	24 ± 2	2.1 ± 0.2	0.98 ± 0.09
	$\mathfrak{S}(02)_{N_2}$ (Å²)		$\mathfrak{S}\binom{02}{20}_{N_2}$ (Å²)	
N_2	61.9 ± 2.2	23.7 ± 0.9	2.77 ± 0.13	1.49 ± 0.05

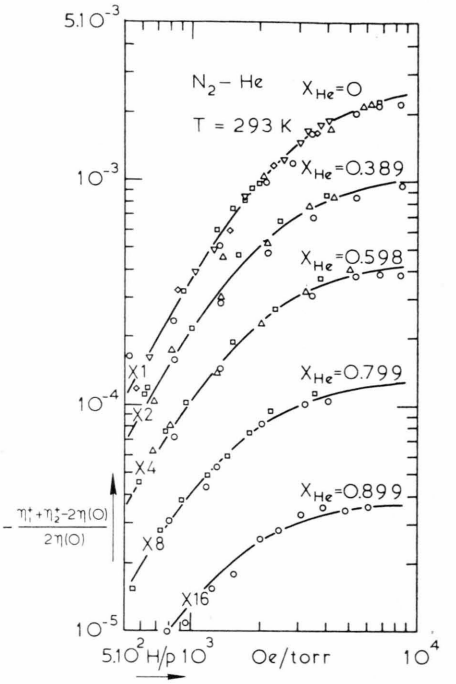

Fig. 9. $-[\eta_1^+ + \eta_2^+ - 2\,\eta(0)]/2\,\eta(0)$ versus H/p for various compositions of the system N_2–He at 293 K. To distinguish the different curves, they are shifted in the vertical direction as in Figure 2.

$x_{He}=0$: ○ 3.61 torr; △ 4.60 torr; ◇ 5.39 torr; ▽ 7.61 torr; □ 15.5 torr.
$x_{He}=0.389$: ○ 3.58 torr; △ 5.89 torr; □ 7.89 torr;
$x_{He}=0.598$: ○ 3.57 torr; △ 6.00 torr; □ 8.25 torr.
$x_{He}=0.799$: ○ 6.08 torr; □ 8.75 torr.
$x_{He}=0.899$: ○ 5.06 torr.
—— theoretical H/p dependence, scaled to the experimental points.

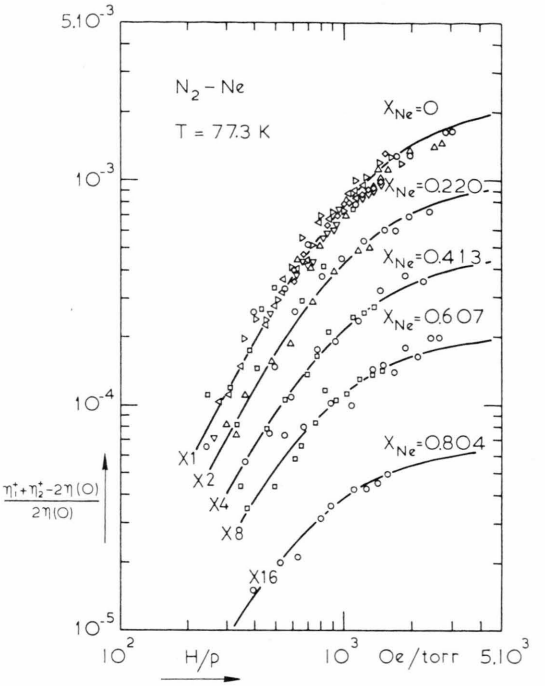

Fig. 10. $-[\eta_1^+ + \eta_2^+ - 2\,\eta(0)]/2\,\eta(0)$ versus H/p for various compositions of the system N_2–Ne at 77.3 K. To distinguish the different curves, they are shifted in the vertical direction as in Figure 2.

$x_{Ne}=0$: ○△▷◇◁▽□ points taken from Figure 8.
$x_{Ne}=0.220$: ○ 1.25 torr; △ 2.13 torr; □ 3.80 torr.
$x_{Ne}=0.413$: ○ 1.32 torr; □ 2.24 torr.
$x_{Ne}=0.607$: ○ 1.13 torr; □ 2.08 torr.
$x_{Ne}=0.804$: ○ 1.96 torr.
—— theoretical H/p dependence, scaled to the experimental points.

4.2. The saturation value as a function of composition

In the theoretical expression for Ψ_{02} [see Eqs. (7) and (8)] nine different cross sections occur, viz., the gas-kinetic cross sections $\mathfrak{S}(20)_A$, $\mathfrak{S}(20)_B$, $\mathfrak{S}(^{20A}_{20A})_{AB}$, $\mathfrak{S}(^{20B}_{20B})_{AB}$ and $\mathfrak{S}(^{02A}_{02B})_{AB}$, the reorientation cross sections $\mathfrak{S}(02)_A$ and $\mathfrak{S}(^{02A}_{02A})_{AB}$ and the coupling cross sections $\mathfrak{S}(^{02}_{20})_A$ and $\mathfrak{S}(^{02A}_{20A})_{AB}$.

Of the five gas-kinetic cross sections, two are known from the field free viscosity of the pure gases, i. e.,

$$\mathfrak{S}(20)_A = \frac{1}{\langle v_A\rangle_0}\frac{kT}{\eta_A(0)}$$

and

$$\mathfrak{S}(20)_B = \frac{1}{\langle v_B\rangle_0}\frac{kT}{\eta_B(0)}. \qquad (13)$$

In principle the other three quantities can be determined from the field free viscosity of the mixture, which is given by:

$$\eta(0) = \tfrac{1}{2}\,kT\,(x_A\,B_A^{20} + x_B\,B_B^{20})\,. \qquad (14)$$

Since little viscosity data are available for mixtures we wil calculate the cross sections

$$\mathfrak{S}(^{20A}_{20A})_{AB}, \quad \mathfrak{S}(^{20B}_{20B})_{AB} \quad \text{and} \quad \mathfrak{S}(^{20A}_{20B})_{AB}.$$

This can be done with great accuracy as these quantities are mainly determined by the spherical part of the intermolecular interaction, so that one can relate them to the well known Ω-integrals (see e. g. Ref. [18]). Thus one gets:

$$\mathfrak{S}(^{20A}_{20A})_{AB} = \frac{8\,m_B}{(m_A+m_B)^2}\cdot\left\{\tfrac{1}{5}m_B\,\Omega^{(2,2)^*}_{AB} + \tfrac{1}{3}m_A\,\Omega^{(1,1)^*}_{AB}\right\}\pi\,\sigma_{AB}^2, \qquad (15)$$

$$\mathfrak{S}(^{20B}_{20B})_{AB} = \frac{8\,m_A}{(m_A+m_B)^2}\cdot\left\{\tfrac{1}{5}m_A\,\Omega^{(2,2)^*}_{AB} + \tfrac{1}{3}m_B\,\Omega^{(1,1)^*}_{AB}\right\}\pi\,\sigma_{AB}^2 \qquad (16)$$

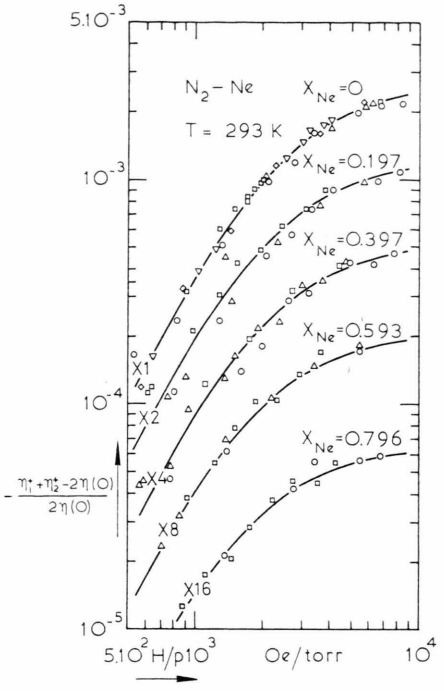

Fig. 11. $-[\eta_1^+ + \eta_2^+ - 2\,\eta\,(0)]/2\,\eta\,(0)$ versus H/p for various compositions of the systems N_2—Ne at 293 K. To distinguish the different curves, they are shifted in the vertical direction as in Figure 2.

$x_{Ne}=0$: ○△▷◇◁▽□ points taken from Figure 9.
$x_{Ne}=0.197$: ○ 3.72 torr; △ 5.33 torr; □ 8.03 torr.
$x_{Ne}=0.397$: ○ 3.85 torr; △ 5.16 torr; □ 7.02 torr.
$x_{Ne}=0.593$: ○ 3.46 torr; △ 5.67 torr; □ 8.39 torr.
$x_{Ne}=0.796$: ○ 4.52 torr; □ 7.09 torr.
—— theoretical H/p dependence, scaled to the experimental points.

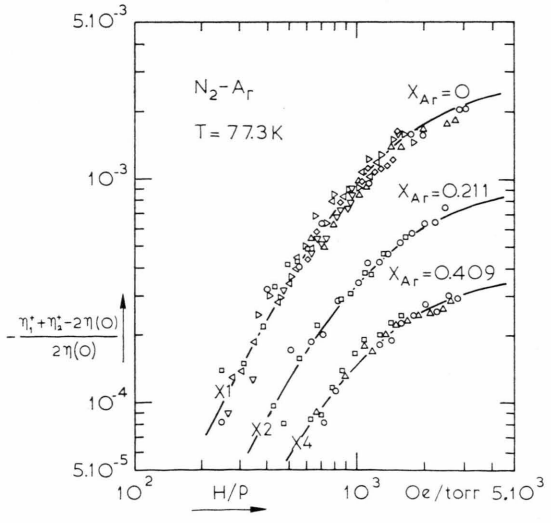

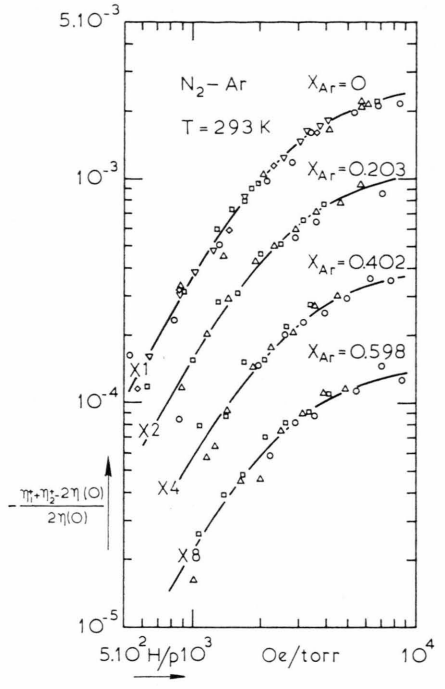

Fig. 13. $-[\eta_1^+ + \eta_2^+ - 2\,\eta\,(0)]/2\,\eta\,(0)$ versus H/p for various compositions of the system N_2—Ar at 293 K. To distinguish the different curves, they are shifted in the vertical direction as in Figure 2.

$x_{Ar}=0$: ○△ ◇ ▽□ points taken from Figure 9.
$x_{Ar}=0.203$: ○ 3.42 torr; △ 5.39 torr; □ 7.81 torr.
$x_{Ar}=0.402$: ○ 3.90 torr; △ 5.44 torr; □ 7.33 torr.
$x_{Ar}=0.598$: ○ 3.46 torr; △ 6.23 torr; □ 7.42 torr.
—— theoretical H/p dependence, scaled to the experimental points.

and

$$\mathfrak{S}\left(\begin{smallmatrix}20A\\20B\end{smallmatrix}\right)_{AB} = \frac{8\,m_A\,m_B}{(m_A+m_B)^2} \cdot \left\{\tfrac{1}{5}\,\Omega_{AB}^{(2,2)*} - \tfrac{1}{3}\,\Omega_{AB}^{(1,1)*}\right\} \pi\,\sigma_{AB}^2 \tag{17}$$

where $\sigma_{AB} = \frac{1}{2}\,(\sigma_A + \sigma_B)$ with σ_A and σ_B the Lennard-Jones diameters of molecules A and B, respectively.

The two reorientation cross sections $\mathfrak{S}(02)_A$ and $\mathfrak{S}\left(\begin{smallmatrix}02A\\02A\end{smallmatrix}\right)_{AB}$ have already been discussed in Section 4.1 and are given in Table 2.

Fig. 12. $-[\eta_1^+ + \eta_2^+ - 2\,\eta\,(0)]/2\,\eta\,(0)$ versus H/p for various compositions of the system N_2—Ar at 77.3 K. To distinguish the different curves, they are shifted in the vertical direction as in Figure 2.

$x_{Ar}=0$: ○△▷◇◁▽□ points taken from Figure 8.
$x_{Ar}=0.211$: ○ 1.22 torr; □ 1.85 torr.
$x_{Ar}=0.409$: ○ 1.06 torr; △ 1.14 torr; □ 1.98 torr.
—— theoretical H/p dependence, scaled to the experimental points.

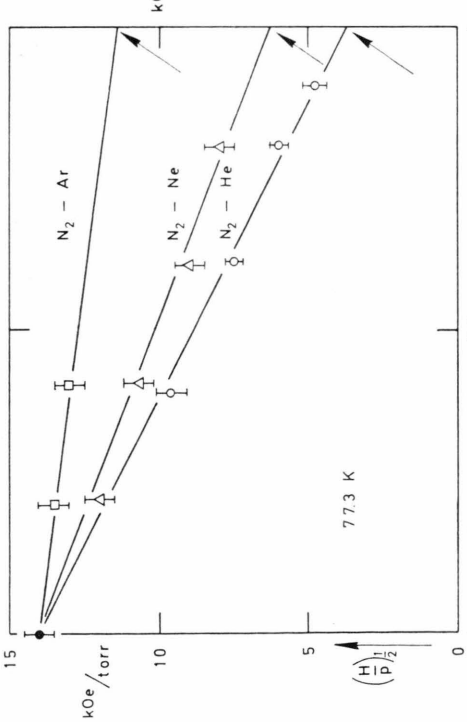

Fig. 14. The values for $(H/p)_{1/2}$ versus the mole fraction of the noble gas for the systems HD−He, HD−Ne and HD−Ar at 77.3 K. By extrapolating the fitted straight lines [Eq. (4)] to $x_{\text{noble gas}}=1$, values are obtained for the cross sections $\mathfrak{S}\left(^{02\text{HD}}_{02\text{HD}}\right)$ HD-n.g..

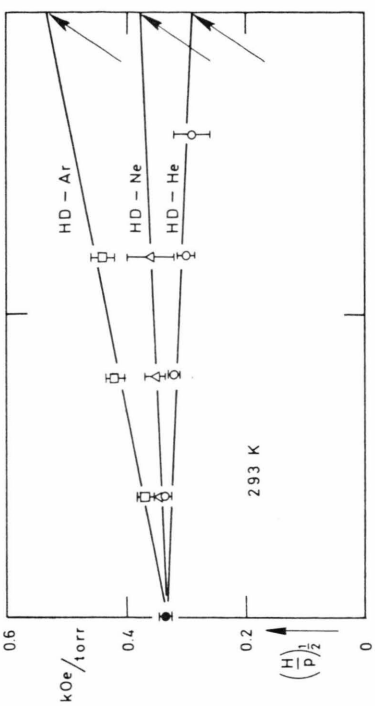

Fig. 15. The values for $(H/p)_{1/2}$ versus the mole fraction of the noble gas for the systems HD−He, HD−Ne and HD−Ar at 293 K. By extrapolating the fitted straight lines [Eq. (4)] to $x_{\text{noble gas}}=1$, values are obtained for the cross sections $\mathfrak{S}\left(^{02\text{HD}}_{02\text{HD}}\right)$ HD-n.g..

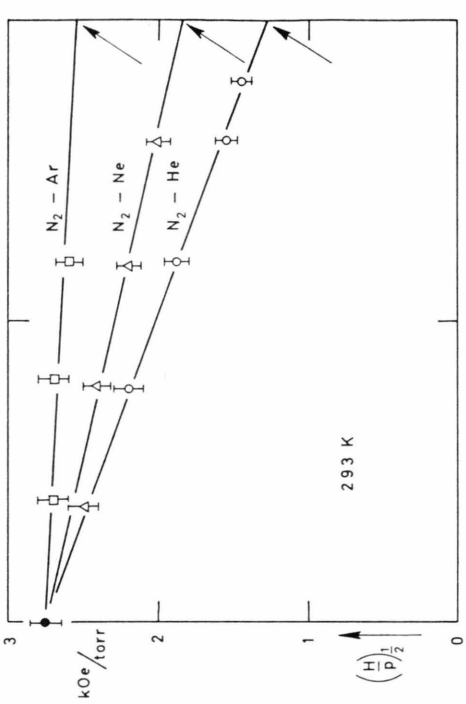

Fig. 17. The values for $(H/p)_{1/2}$ versus the mole fraction of the noble gas for the systems N_2−He, N_2−Ne and N_2−Ar at 293 K. By extrapolating the fitted straight lines [Eq. (4)] to $x_{\text{noble gas}}=1$, values are obtained for the cross sections $\mathfrak{S}\left(^{02\text{N}_2}_{02\text{N}_2}\right)$ N_2-n.g..

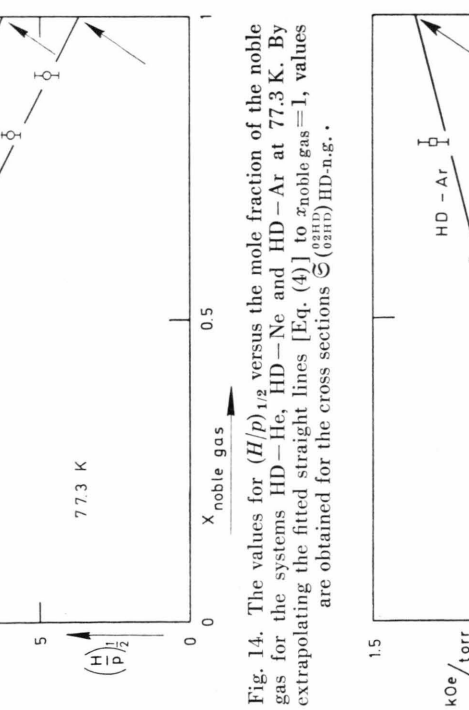

Fig. 16. The values for $(H/p)_{1/2}$ versus the mole fraction of the noble gas for the systems N_2−He, N_2−Ne and N_2−Ar at 77.3 K. By extrapolating the fitted straight lines [Eq. (4)] to $x_{\text{noble gas}}=1$, values are obtained for the cross sections $\mathfrak{S}\left(^{02\text{N}_2}_{02\text{N}_2}\right)$ N_2-n.g..

Of the two coupling cross sections $\mathfrak{S}\left(^{02}_{20}\right)_{\text{A}}$ and $\mathfrak{S}\left(^{02\text{A}}_{20\text{A}}\right)_{\text{AB}}$, the magnitude of the quantity $\mathfrak{S}\left(^{02}_{20}\right)_{\text{A}}$ is known from experiments on the field effect in pure gases, while the sign can be determined from measurements on streaming birefringence. Such experiments have been performed for N_2 [19] and recently also for HD [20]. In both cases the sign is found to be positive. The cross section $\mathfrak{S}\left(^{02\text{A}}_{20\text{A}}\right)_{\text{AB}}$ is the only re-

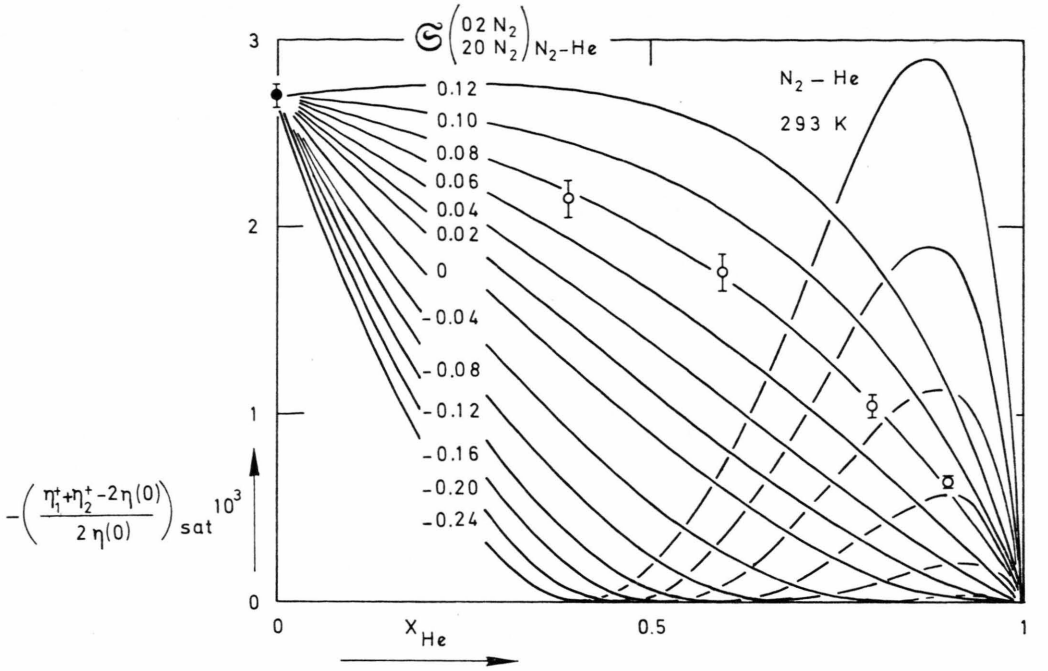

Fig. 18. The theoretical saturation values, Ψ_{02} of $-[\eta_1^+ + \eta_2^+ - 2\eta(0)]/2\eta(0)$ versus the mole fraction of He for the system N_2–He at 293 K, calculated from Eq. (7) for various values of $\mathfrak{S}\left(\begin{matrix}02N_2\\20N_2\end{matrix}\right)_{N_2\text{-}He}$. The best agreement with the experimental points is found for $\mathfrak{S}\left(\begin{matrix}02N_2\\20N_2\end{matrix}\right)_{N_2\text{-}He} = +0.08$ Å².

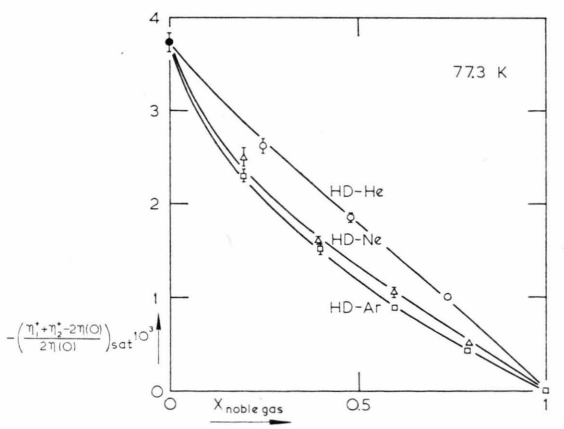

Fig. 19. The saturation values of $-[\eta_1^+ + \eta_2^+ - 2\eta(0)]/2\eta(0)$ versus the mole fraction of the noble gas for the systems HD–He, HD–Ne and HD–Ar at 77.3 K. The solid lines are given by Eq. (7) using the value of $\mathfrak{S}\left(\begin{matrix}02HD\\20HD\end{matrix}\right)_{HD\text{-n.g.}}$ which gives the best fit of the experimental points.

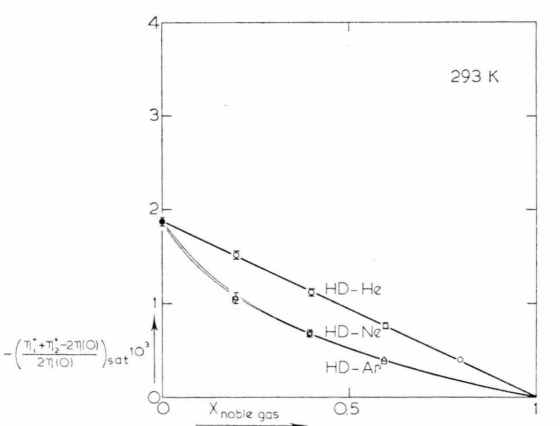

Fig. 20. The saturation values of $-[\eta_1^+ + \eta_2^+ - 2\eta(0)]/2\eta(0)$ versus the mole fraction of the noble gas for the systems HD–He, HD–Ne and HD–Ar at 293 K. The solid lines are given by Eq. (7) using the value of $\mathfrak{S}\left(\begin{matrix}02HD\\20HD\end{matrix}\right)_{HD\text{-n.g.}}$ which gives the best fit of the experimental points.

maining quantity in Eq. (7) which is not yet known and is therefore determined from the experiments reported here. Figure 18 gives the theoretical curves and experimental points for the saturation value Ψ_{02} as a function of noble gas mole fraction. The theoretical curves are calculated with various values of $\mathfrak{S}\left(\begin{matrix}02N_2\\20N_2\end{matrix}\right)_{N_2\text{-}He}$ both positive and negative. It is obvious that good agreement between theory and experiment can be obtained for

$$\mathfrak{S}\left(\begin{matrix}02N_2\\20N_2\end{matrix}\right)_{N_2\text{-}He} = +0.080\ \text{Å}^2.$$

Note that Eq. (7) gives the same results if the sign of both $\mathfrak{S}\left(\begin{matrix}02\\20\end{matrix}\right)_{N_2}$ and $\mathfrak{S}\left(\begin{matrix}02N_2\\20N_2\end{matrix}\right)_{N_2\text{-}He}$ is changed, because of the square in the numerator so that in fact

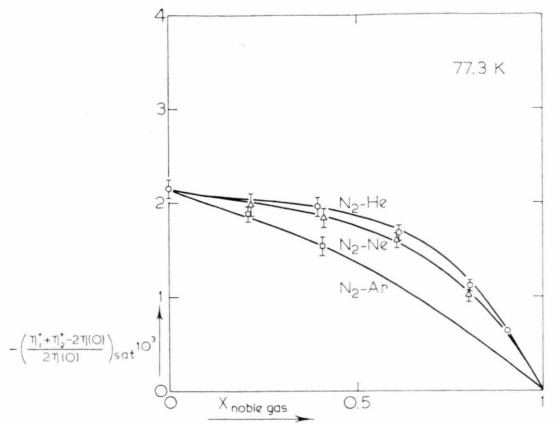

Fig. 21. The saturation values of $-[\eta_1^+ + \eta_2^+ - 2\eta(0)]/2\eta(0)$ versus the mole fraction of the noble gas for the systems N_2-He, N_2-Ne and N_2-Ar at 77.3 K. The solid lines are given by Eq. (7) using the value of $\Im\binom{02N_2}{20N_2}_{N_2\text{-n.g.}}$ which gives the best fit of the experimental points.

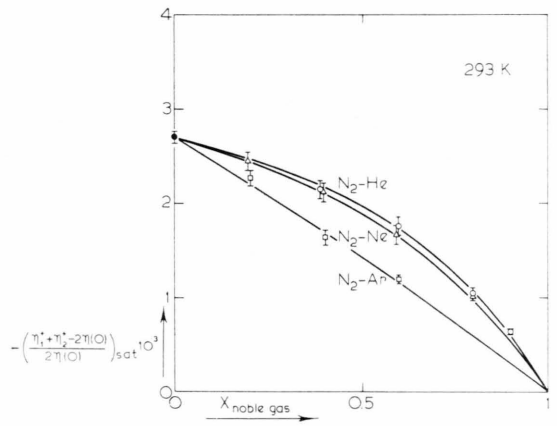

Fig. 22. The saturation values of $-[\eta_1^+ + \eta_2^+ - 2\eta(0)]/2\eta(0)$ versus the mole fraction of the noble gas for the systems N_2-He, N_2-Ne and N_2-Ar at 293 K. The solid lines are given by Eq. (7) using the value of $\Im\binom{02N_2}{20N_2}_{N_2\text{-n.g.}}$ which gives the best fit of the experimental points.

one can conclude from our experiments that both coupling cross sections have the same sign. For all mixtures such plots are made and always good agreement between theory and experiment is found for a given value of $\Im\binom{02A}{20A}_{AB}$. Moreover, the sign of $\Im\binom{02A}{20A}_{AB}$ is always the same as that of $\Im\binom{02}{20}_A$.

In Figs. 19 to 22 the results for all investigated systems are shown, along with the theoretical curve which gives best agremeent with the experimental data. The various parameters used in these calculations were obtained from Refs. [21–24] and are summarized in Table 3. In Table 2 the values of $\Im\binom{02A}{20A}_{AB}$ used in obtaining these curves are given together with te values of $\Im\binom{02}{20}_A$. It is seen that the production of $[\boldsymbol{J}_A]^{(2)}$ polarization from a

Table 3. Summary of the parameters used in the calculations.

	ε/k (K)	σ (Å)	$\eta(0)$ (μP) 77.3 K	293 K
He	10.22	2.556	83	196
Ne	34.9	2.780	120	312
Ar	119.8	3.405	66	223
HD	37.0	2.928	42	107
N_2	91.5	3.681	54	174

$[\boldsymbol{W}_A]^{(2)}$ polarization through interactions A – B is more effective for heavier or larger noble gas molecules. In all the cases of N_2-noble gas mixtures which have been investigated, it is found that the noble gas is always less effective than N_2 in producing $[\boldsymbol{J}_A]^{(2)}$ polarization. The quantity $\Im\binom{02}{20}_{HD}$ at both temperatures lies between $\Im\binom{02HD}{20HD}_{HD-He}$ and $\Im\binom{02HD}{20HD}_{HD-Ne}$. At 77 K the cross sections $\Im\binom{02A}{20A}_{AB}$ are all larger than their corresponding values at 293 K, while the relative increase with temperture is larger for heavier noble gas molecules.

Acknowledgements

The authors wish to express their sincere thanks to Prof. J. J. M. Bennakker for his interest and support in this work and Dr. J. Korving for making available his personal notes concerning the theory of the viscomagnetic effect for mixtures.

This work is part of the research program of the "Stichting voor Fundamenteel Onderzoek der Materie (F.O.M.)" and has been made possible by financial support from the "Nederlandse Organisatie voor Zuiver Wetenschappelijk Onderzoek (Z.W.O.)".

[1] A. L. J. Burgmans, P. G. van Ditzhuyzen, H. F. P. Knaap, and J. J. M. Beenakker, Z. Naturforsch. **28 a**, 835 [1973].
[2] J. A. R. Coope and R. F. Snider, J. Chem. Phys. **56**, 2056 [1972].
[3] S. R. De Groot and P. Mazur, Non-equilibrium Thermodynamics, North-Holland Publishing Comp., Amsterdam 1962, p. 311.
[4] H. Moraal, F. R. McCourt, and H. F. P. Knaap, Physica **45**, 455 [1969] (Commun. Kamerlingh Onnes Lab., Leiden, Suppl. No. 127 d).
[5] H. Hulsman and A. L. J. Burgmans, Phys. Letters **29 A**, 629 [1969].
[6] H. Hulsman, E. J. van Waasdijk, A. L. J. Burgmans, H. F. P. Knaap, and J. J. M. Beenakker, Physica **50**, 53 [1970] (Commun. Kammerlingh Onnes Lab., Leiden No. 381 c).

[7] H. Hulsman, F. G. van Kuik, K. W. Walstra, H. F. P. Knaap, and J. J. M. Beenakker, Physica **57**, 501 [1972] (Commun. Kamerlingh Onnes Lab., Leiden No. 389 a).
[8] J. Korving, Physica, to be published.
[9] J. J. M. Beenakker and F. R. McCourt, Ann. Rev. Phys. Chem. **21**, 47 [1970]; J. J. M. Beenakker, H. F. P. Knaap, and B. C. Sancturary, American Institute of Physics — Conference and Symposium series, Vol. **11** [1973].
[10] A. Tip, Physica **37**, 411 [1967].
[11] H. H. Raum and W. E. Köhler, Z. Naturforsch. **25 a**, 1178 [1970].
[12] G. J. Prangsma, A. L. J. Burgmans, H. F. P. Knaap, and J. J. M. Beenakker, Physica, to be published [1973].
[13] F. R. McCourt and H. Moraal, Chem. Phys. Letters **9**, 39 [1971].
[14] A. C. Levi, F. R. McCourt, and A. Tip, Physica **39**, 165 [1968] (Commun. Kamerlingh Onnes Lab., Leiden, Suppl. No. 126 b).
[15] J. Korving, H. Hulsman, G. Scoles, H. F. P. Knaap, and J. J. M. Beenakker, Physica **36**, 177 [1967] (Commun. Kamerlingh Onnes Lab., Leiden No. 357 b).
[16] L. B. Loeb, The Kinetic Theory of Gases, McGraw-Hill Book Cy., Inc., New York and London 1934, p. 297.
[17] S. Chapman and T. G. Cowling, The Mathematical Theory of Non-uniform Gases, Cambridge University Press, London 1970, p. 88.
[18] S. Chapman and T. G. Cowling, The Mathematical Theory of Non-uniform Gases, Cambridge University Press, London 1970, p. 159.
[19] F. Baas, Phys. Letters **36 A**, 107 [1971].
[20] F. Baas, private communication.
[21] J. O. Hirschfelder, C. F. Curtiss, and R. B. Bird, The Molecular Theory of Gases and Liquids, John Wiley and Sons Inc., New York 1954, p. 1110.
[22] Data Book, edited by Thermophysical Properties Research Center, Purdue University, Lafayette, Indiana 1966, Vol. 2.
[23] A. O. Rietveld, A. van Itterbeek, and C. A. Velds, Physica **25**, 205 [1959] (Commun. Kamerlingh Onnes Lab., Leiden No. 314 b).
[24] A. O. Rietveld and A. van Itterbeek, Physica **22**, 785 [1956] (Commun. Kamerlingh Onnes Lab., Leiden No. 304 e).

Heat-Flow Birefringence in Gases

S. Hess

Institut für Theoretische Physik der Universität Erlangen-Nürnberg, Erlangen

(Z. Naturforsch. **28 a**, 861 – 868 [1973]; received 7th September 1972)

Dedicated to Prof. Dr. L. Waldmann on the occasion of his 60th birthday

Heat-flow birefringence is described by a constitutive law which links the anisotropic part of the dielectric tensor with the gradient of the heat flux or the 2nd spatial derivative of the temperature field. For a gas of linear molecules, this relation is derived from transport-relaxation equations which, in turn, were obtained from the Waldmann-Snider equation. The magnitude of the heat-flow birefringence can be inferred from the Senftleben-Beenakker effect of the viscosity and of the heat conductivity. It is found to be of measurable size.

Transport processes in a fluid of optically anisotropic particles may lead to a birefringence, i. e. its dielectric tensor may possess a nonvanishing anisotropic part. Flow birefringence [1, 2] and acoustic birefringence [2, 3] are examples for such nonequilibrium birefringence phenomena. Both effects are described by a constitutive law which links the anisotropic part of the dielectric tensor with the gradient of the velocity. In a heat-conducting fluid the anisotropic part of the dielectric tensor can be proportional to the gradient of the heat flux or equivalently to the 2-nd spatial derivative of the temperature. A kinetic theory of this "heat-flow birefringence" is presented for gases of rotating molecules.

In contradistinction to liquids and colloidal solutions where birefringence is due to an alignment of the figure axis of the particles, in gases of rotating molecules it is connected with an alignment of the molecular rotational angular momentum [4]. This is reflected by the fact that the anisotropic part of the dielectric tensor is proportional to the tensor polarization of the rotational angular momentum. For the theoretical treatment of nonequilibrium birefringence phenomena the collision-induced tensor polarization has to be studied. Point of departure for such a theory is the Waldmann-Snider equation [5, 6], a generalized Boltzmann equation for particles with internal rotational degrees of freedom. Waldmann [5] mentioned flow birefringence as a possible application of his kinetic equation as early as 1957. The kinetic theory of flow birefringence, however, has been developed much later [7, 8]. This paper deals with the theory of the heat-flow birefringence. Its magnitude can be inferred from measurements of the influence of magnetic fields on the heat conductivity and the viscosity [9, 10] (Senftleben-Beenakker effect). It turns out to be of similar size as the flow birefringence in gases which has recently been observed experimen-